Article

Water-Induced Negative Electron Affinity on Diamond (100)

Xingyu Gao, Lei Liu, Dongchen Qi, Shi Chen, A. T. S. Wee, Ti
Ouyang, Kian Ping Loh, Xiaojiang Yu, and Herbert O. Moser

More About This Article

Additional resources and features associated with this article are available within the HTML version:

- Supporting Information
- Access to high resolution figures
- Links to articles and content related to this article
- Copyright permission to reproduce figures and/or text from this article

View the Full Text HTML

Water-Induced Negative Electron Affinity on Diamond (100)

Xingyu Gao,* Lei Liu, Dongchen Qi, Shi Chen, and A. T. S. Wee

Physics Department, National University of Singapore, 2 Science Drive 3, Singapore 117542, Republic of Singapore

Ti Ouyang and Kian Ping Loh

Department of Chemistry, National University of Singapore, 3 Science Drive 3, Singapore 117543, Republic of Singapore

Xiaojiang Yu and Herbert O. Moser

Singapore Synchrotron Light Source, National University of Singapore, 5 Research Link, Singapore 117603, Republic of Singapore

The interaction of water vapor on clean diamond (100) has been studied using ultraviolet photoemission spectroscopy (UPS), X-ray photoemission spectroscopy (XPS), X-ray-absorption near-edge structure (XANES) spectroscopy, and high-resolution electron energy loss spectroscopy (HREELS). It is shown that water dissociates at room temperature on clean diamond forming C−H and C−OH bonds, resulting in a surface dipole layer which produces the condition of negative electron affinity (NEA). The strong polarization dependence of the O *K* XANES could be associated with the out-of-plane orientation of the OH bonds. Density functional theory (DFT) calculations confirm the existence of NEA on this surface with a mixture of hydrogen and hydroxyl (OH) terminations.

Diamond has emerged as an important technological material for high power transistor and UV photo detector applications owing to its wide band gap. In the area of biomedicine, there are reports on the advantages of using diamond as a platform for the immobilization of biomolecules due to its biocompatibility and stable interface.[1−4] In most of these applications, the surface condition of diamond, in terms of its hydrophobic or hydrophilic character after different surface termination, can affect its surface processing and electrical performance. Hydrogenated diamond surface is known to exhibit unique properties such as negative electron affinity (NEA)[5−7] and p-type surface conductivity (SC),[9−12] which are useful for device applications in field emitters and ion-selective field effect transistors.[13−17] It has been shown that the p-type surface conductivity on nominally undoped diamond observable in humid air can be attributed to the influence of hydroxonium ions, arising from the interaction of water with surface hydrogen.[18−21] The so-called "surface transfer doping" model explains the transfer of valence band electrons from diamond to the high electron affinity hydroxonium ions, giving rise to hole accumulation.[18−21] While there are many studies to explain the origin of p-type surface conductivity, few studies focus on specifically the reaction of water with diamond.[22−24] Water is an industrially important reagent in microelectronic processing; for example, it can act as an oxidizing agent in the growth of silicon oxide on silicon. The wetting of the hydrophobic diamond surface by water can result in gradual hydroxylation of the diamond surface in the ambient. In this paper, we study the interaction of water vapor with clean diamond (100) to understand the chemistry of water dissociation as well as its

effects on the electronic properties of diamond. HREELS (High-resolution electron energy loss) measurements show that the dissociation of water produced C−H and C−OH groups on the diamond surface. Density functional theory (DFT) calculations indicate that a mixture of CH and OH groups on the diamond surface can provide an even larger NEA than that of hydrogenated diamond, making it potentially useful for NEA based applications.

A boron-doped p-type single-crystal diamond (100) sample with a doping concentration of 100 ppm was used in this study. It was hydrogenated at 800 °C for 10 min in a hydrogen plasma microwave (800 W) chamber at an operating pressure of 20 mbar. For high-resolution electron energy loss spectroscopy (HREELS) measurements, the sample was transferred in situ into an ultrahigh vacuum (UHV) chamber with a base pressure of 5×10^{-11} mbar. For synchrotron measurements, it was quickly transferred ex situ into the UHV chamber at the SINS beamline[25] of the Singapore synchrotron light source (SSLS) with a base pressure of better than 1×10^{-10} mbar, minimizing exposure to air during the transfer to several hours. A sharp (2×1) low-energy electron diffraction (LEED) pattern was observed after the sample was annealed at about 100 °C overnight in UHV, indicating that the hydrogenated diamond surface is stable and can be easily recovered in UHV after sample transfer. After the measurements on the hydrogenated surface, the sample was annealed to 1100 °C to revert it to the clean diamond surface. The diamond surface was exposed to water vapor in the respective preparation chambers through precision leak valves at room temperature. After exposure, the sample was transferred in situ to the main chambers for HREELS and synchrotron measurements respectively.
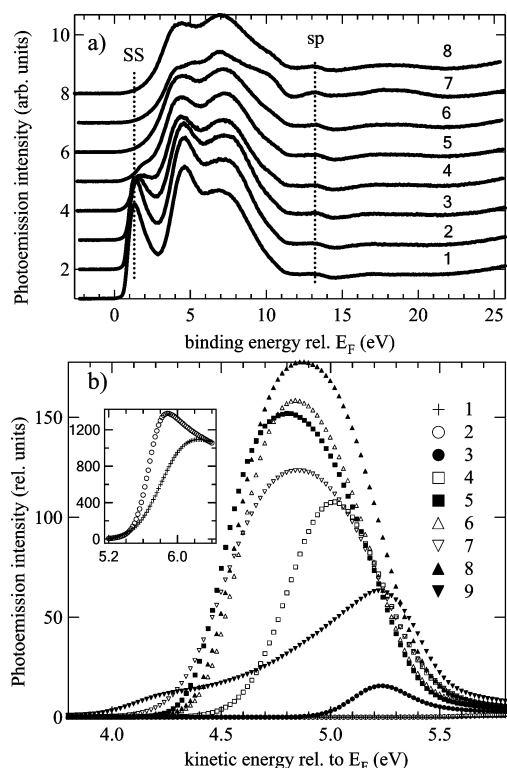
* Corresponding author.

2488 *J. Phys. Chem. C, Vol. 112, No. 7, 2008*

Gao et al.

Figure 1. Valence band spectra (a) and the low kinetic energy part of the UPS spectra (b) for diamond surface at different conditions: bare diamond (1), bare diamond after water dosage of 200 L (2), 1200 L (3), 3200 L (4), 10 000 L (5), and 100 000 L (6) at room temperature. Spectra (7) were recorded after the maximum dosage described in the text, and spectra (8) were obtained with the diamond further annealed to 300 °C in UHV condition for 10 min. Spectrum (9) was for the hydrogenated diamond as reference. All spectra were recorded at normal emission with photon energy of 60 eV. Notice the different scales of the inset in b.

Photoemission and X-ray absorption spectroscopy (XAS) were performed using p-polarized light with the photon energy resolution $E/\Delta E$ set at about 1000, and a hemispherical electron energy analyzer (EA 125, Omicron NanoTechnology GmbH). The XAS spectra were measured using both sample drain current in total electron yield (TEY) mode and O KVV Auger electrons detected by the analyzer in Auger electron yield (AEY) mode simultaneously. The photon beam and the analyzer are in the horizontal plane with a fixed angle of 50° between the incident light and the detected electrons. The sample can be rotated about the vertical axis to change the emission angle and incidence angle. The HREELS measurements were performed using a SPECS spectrometer ECU 500D, and the spectra were measured in specular geometry with 6 eV primary electron energy.

Figure 1 shows the valence band UPS spectra (a) and its low kinetic energy cutoff (b) from diamond (001) with normal electron emission angle at room temperature after exposure to water vapor at different dosages and conditions. The spectra in Figure 1b were measured with a negative sample bias of 5 V to eliminate the influence of the analyzer work function. The kinetic energy scale in b is after the deduction of this bias and is therefore referenced to the Fermi level of the sample. The maximum dosage in the experiments was achieved by exposing the sample in the load lock at water vapor pressure about atmosphere for over 10 min and then pumping down to a base pressure of several 10^{-9} mbar. From Figure 1a, there is an obvious decrease in the peak labeled SS with increasing water dosage, and this peak disappears completely in spectrum 6 at a dosage of 100 000 L. At the same time, the secondary electron
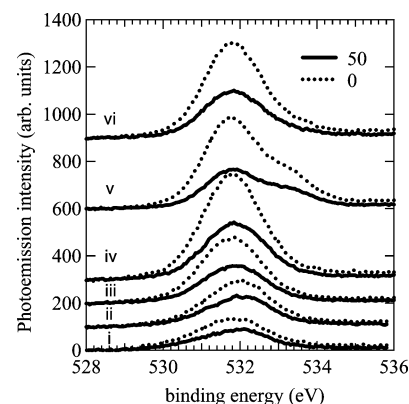

Figure 2. O 1s photoemission spectra with photon energy of 625 eV at emission angles of 50° (solid line) and 0° (dashed line) for diamond (001) at different water dosages and conditions: water dosage of 1200 L (i), 3200 L (ii), 10 000 L (iii), 100 000 L (iv), maximum dosage as described in text (v), and annealed at 300 °C for 10 min after maximum dosage of water (vi).
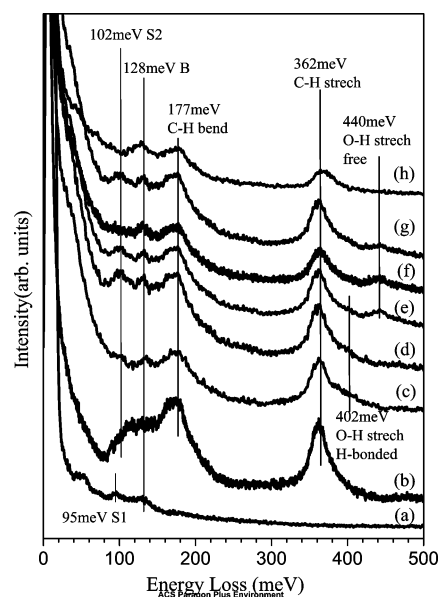

Figure 3. HREELS measured after different treatments: (a) bare diamond surface, (b) right after dosing water, and after subsequent annealing to (c) 100 °C, (d) 200 °C, (e) 300 °C, (f) 400 °C, (g) 500 °C, and (h) 600 °C.

emission intensity from diamond increases with the water dosage, and the low-energy cutoff decreases as shown in Figure 1b. It is well-known that the peak SS at around 1.3 eV in Figure 1a represents the dimer π bond induced surface state.[26] While the peak at 13 eV which is a fingerprint of sp^3 bonding in bulk single crystalline diamond is only slightly attenuated, the gradual decrease of the SS peak directly indicates a chemical reaction on diamond that breaks the dimer π bonds rather than a simple attenuation of the photoemission intensity due to adsorbed water layers. This conclusion is confirmed by our HREELS results (Figure 3). Therefore, changes in the secondary electron emission should be a direct consequence of the chemical reaction of water with the clean diamond surface. By comparing the changes due to water dosage in Figure 1a,b, it is noted that the rate of change of the SS peak height is correlated to those of both the secondary electron peak height and the low kinetic energy cutoff position. When the SS peak disappears completely at a dosage of 100 000 L, the secondary electron peak height reaches its maximum with the low kinetic energy cutoff down to its minimum (see spectra 6 in Figure 1). At this stage, a

Negative Electron Affinity on Diamond (100)

J. Phys. Chem. C, Vol. 112, No. 7, 2008 **2489**

TABLE 1: Summary of Work Function ϕ, C 1s Binding Energy, CBM Position Relative to Fermi Level $E_c - E_F$, VBM Position Relative to Fermi Level $E_v - E_F$, Band Bending E_{BB}, and Electron Affinity χ for Different Surface Conditions[a]

surface	ϕ (eV)	C 1s (eV)	$E_c - E_F$ (eV)	$E_v - E_F$ (eV)	E_{BB} (eV)	χ (eV)
bare	5.5	284.6	4.8	−0.7	−0.4	0.7
1200 L	4.9	284.5	5.0	−0.5	−0.3	0.0
3200 L	4.6	284.4	5.0	−0.5	−0.2	−0.4
10 000 L	4.3	284.3	5.1	−0.4	−0.1	−0.8
100 000 L	4.4	284.3	5.1	−0.4	−0.1	−0.7
maximum	4.3	284.3	5.1	−0.4	−0.1	−0.8
annealed	4.3	284.4	5.1	−0.4	−0.2	−0.7
hydrogenated	4.0	284.5	4.9	−0.6	−0.3	−1.0

[a] The negative sign of E_{BB} refers to a downward band bending.

complete layer of dissociated water species on diamond is formed, and further dosage causes a decrease in the secondary electron peak. The UPS spectrum 7 with maximum water dosage in Figure 1a shows additional structures (for example, the rising bump at about 10 eV), suggesting that further dosage introduces additional adsorbates. These adsorbates appear to be the reason for the decrease in the secondary electron peak. After a mild annealing at 300 °C, the UPS spectrum 8 reverts to that of spectrum 6 with an even higher NEA peak; this is attributed to the removal of these new adsorbates. Although the hydrogenated surface still has the lowest kinetic energy cutoff corresponding to the lowest vacuum level, the strongest NEA peak as shown in Figure 1b is achieved after maximum water dosage and subsequent mild annealing (about three times of that from the hydrogenated surface).

To determine the value of electron affinity, which is defined as the energy separation between the conduction band minimum (E_c) and the vacuum level (E_{vac}), we refer to the method described by Cui et al. in ref 7 and Maier et al. in ref 8. As E_{gap} is known to be 5.5 eV, we can use $E_c - E_F = E_{gap} - (E_F - E_v)$ to determine the position of E_c relative to the Fermi level (E_F). Although the diamond valence band maximum (E_v) is not directly visible in the UPS valence band spectra, its energy separation from the C 1s of diamond bulk component in XPS is constant, and hence the position of the VBM can be deduced.[7,8] This energy separation was derived from an independent calibration experiment to be 283.9 eV, with an uncertainty of 0.1 eV.[7,8] We have measured the C 1s binding energy of bulk diamond at different surface conditions, and thus we are able to deduce $E_c - E_F$ accordingly. From the low kinetic energy cut-offs (work function ϕ) in Figure 1b obtained by extrapolation of the secondary electron peak at the low kinetic energy side to zero intensity, the position of the vacuum level E_{vac} at different dosages can be derived.[27] As the position of E_c and E_v in the bulk is known with Fermi level calculated at 0.3 eV above E_v,[7,8] we can also calculate the band bending E_{BB} on the surface. The values of ϕ, C 1s binding energy, $E_c - E_F$, $E_v - E_F$, E_{BB}, and χ for different surface conditions are summarized in Table 1 with an uncertainty of 0.1 eV. The electron affinity values obtained for hydrogenated and bare diamond surfaces are consistent with those in the literature which report χ ranging from −0.4 to −1.3 eV for hydrogenated diamond (001) and 0.5 to 1.3 eV for bare diamond (001).[8] It is clear that water on diamond surfaces induces NEA. With the increase in water dosage, the electron affinity goes down to about −0.8 eV at the saturation dosage. After mild annealing, NEA still remains at about −0.7 eV. With the help of Table 1, it is clear that photoemission can be observed between the vacuum level and the conduction band minimum (CBM) shown in Figure 1b for all of the surfaces with NEA. The photoemission within the band gap could come from either inelastic scattering at the surface to the vacuum interface or more likely the transitions

of electrons from the CBM to unoccupied surface states, as discussed by Diederich et al. for hydrogenated diamond surfaces in ref 28.

To understand the origin of the NEA induced by water adsorption on the diamond surface, we need to identify the species formed on the diamond surface after water adsorption. Water is known to dissociate into H and OH groups on many surfaces.[29,30] On diamond (100), OH groups were found from IR experiments by Struck et al. to be further dissociated into C−O−C (either) or C=C (carbonyl) species at elevated temperature.[22] Laikhtman and co-workers report the formation of C=O, C−O−H, and C−H surface bonds at both room and elevated temperatures using RHEELS.[24] To identify the surface species, we measured the O 1s photoemission spectra at different water dosages and conditions, and the results are summarized in Figure 2. There appears to be almost a single peak at about 532 eV, which is assigned to hydroxyl (−OH) groups from the study of oxygen on diamond surfaces by Makau et al.,[31] for exposures up to 100 000 L. After the maximum dosage at about atmospheric pressure, a shoulder at about 533 eV appears, which may be attributed to oxygen in physisorbed water molecules. Compared with the main peak, this shoulder has a relatively higher intensity at grazing angle than that at normal emission, supporting its assignment as physisorbed water on top of the chemisorbed layer. After mild annealing at 300 °C for 10 min, this shoulder disappears because of the desorption of physisorbed water, and only the main peak at 531.8 eV remains.

HREELS offers additional insight into the surface bound species following the dissociation of water on clean diamond. In the HREELS experiments, clean diamond was exposed to water vapor at a pressure of 1×10^{-4} Torr for 1 h at room temperature in a preparation chamber. Figure 3 shows the HREELS spectra. The two peaks observed on bare diamond (a) are assigned to the surface phonon of dimer in-phase bouncing (S1 at 95 meV) and the diamond bulk optical phonon (B at 128 meV).[32] After water exposure (Figure 3b), the spectrum shows strong features due to water adsorption, in particular, the C−H stretching (362 meV) and bending (177 meV). After heating to 100 °C (c in Figure 3), the C−H stretching peak at 362 meV develops a shoulder at the higher energy side. This shoulder at around 402 meV is attributed to −OH stretching, and this shifted to a distinctive peak at 440 meV with additional annealing. The appearance of this OH peak after annealing could be due to the thermal induced desorption of surface physisorbed water molecules which were hydrogen bonded to the surface OH groups initially, and which red-shifted the OH peak into the overlapping C−H band. After annealing, the red-shift was removed and the OH peak became visible. The red shifts of the O−H bond stretching frequencies by hydrogen bonding have been previously reported by Parra et al.[33] Similar to our results, HREELS experiments by Laikhtman et al. show no observable OH vibrational peak immediately
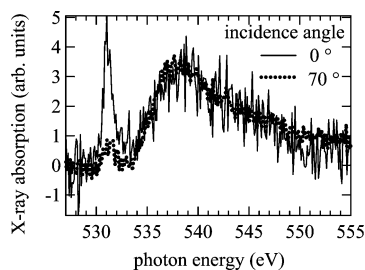
Figure 4. O *K* XANES measured at normal incidence angle (solid line) and an incidence angle of 70 degree (dashed line) using Auger mode.

Figure 5. Calculated plane-averaged, self-consistent potentials of bare, H, 50% OH, and 50% OH + 50% H terminated diamond (100) surfaces diamond (100) surface.

following water adsorption, and the OH peak is observable only after annealing.[24] The observation of OH groups is consistent with the XPS results. As shown, the −OH groups are not stable when annealed at temperatures higher than 500 °C, and the peak disappears after annealing to 600 °C (Figure 3h). We are unable to confirm the presence of C═O groups because of our low sensitivity. C═O peaks observed by Laikhtman and co-workers are also very weak.[24] Combined with our XPS results, we conclude that OH is the main oxygen containing species on diamond after water adsorption. There have been many studies about oxygen on diamond surfaces.[31,34,35] In particular, the study of oxidation of diamond (001) by Pehrsson et al. shows that the distribution of oxygen species varied with oxygen coverage with more hydroxyl species at the initial stage.[35] Water dissociation initially starts from H_2O dissociation into C−H and C−OH;[22] the oxygen coverage on the diamond surface is therefore below half monolayer. According to the study of Skokov and co-workers, the stability of the surface groups is in the order OH > O−C−O > C═O below half monolayer oxygen coverage.[36] Recent DFT calculations on diamond (001) by Sque and co-workers have also show that termination of −OH groups are energetically more favored over a purely oxygenated surface.[37]

X-ray-absorption near-edge structure (XANES) probes the local unoccupied electronic structures with the ability to determine the orientation of different orbitals because of their polarization dependence.[38] We have measured O *K* XANES of the sample after 100 000 L water dosage at both normal and 70° incidence, and the results are presented in Figure 4. It is clear that there is very strong polarization dependence of the first peak located at photon energy of about 531 eV. This peak should not be assigned to the π^* resonance for C═O bond observed at 530 eV by Reinke et al. where they studied ion-irradiated diamond surface and water tends to interact easily with the defects due to the ion irradiation.[23] Our XPS and HREELS results show that oxygen species are mainly OH groups, and we assign this peak to the excitation from O 1s to the partially occupied antibonding π^* orbital of the OH species, which also corresponds to the first peak observed in OH layers at 530 eV on Pt(111) observed by Masanari et al.[39] Amemiya and co-workers also reported a similar peak at 531.5 eV in their O *K*-edge XAS spectra for $CH_3O/Cu(111)$ and $CH_3O/Ni(111)$ systems which was attributed to the partially filled C−O bond.[40] It is thus difficult to determine the origin of this peak. Further theoretical calculations are necessary to interpret the spectra in Figure 4. One possibility is the charge transfer from the substrate C atoms to OH, resulting in partially filled OH bonds with π^* character for the O atom.[39,40] Thus, the strong polarization dependence of this peak could possibly arise from the orientation of the OH species. There could be a $H^+O^-C^+$ double dipole layer on the surface with opposite signs. However, the H atom should lose more electrons than C atoms, and the net dipole

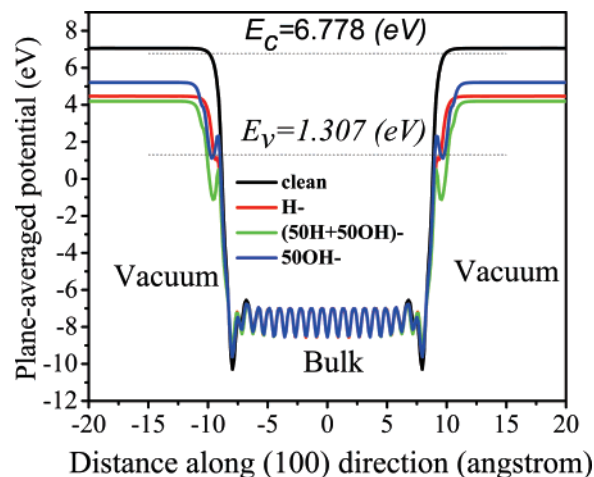layer still tends to bring down the vacuum level and reduce the electron affinity proportionally to the potential step caused by it, according to classical electrostatics.[7] Theoretical DFT calculations by Rutter et al. have also predicted that OH groups on diamond (100) should have NEA.[41] As water dissociates into both H and OH, the dipole layer on the diamond surface comprises a mixture of C−H and O−H species, which should give a different NEA value from that of the hydrogenated surface shown in Table 1.

The lowering of the vacuum level due to water dissociation on the diamond surface is further supported by DFT calculations on clean diamond, H−, 50% OH− and (50% OH + 50% H)-terminated diamond (100) surfaces. The plane wave basis VASP code[42] within the generalized gradient approximation (GGA) was used.[43] The diamond surfaces were modeled by a super-cell containing 20 layers of diamond and a 20 Å vacuum region, to avoid interactions between periodically repeated slabs. Both surfaces of the slab were kept equivalent; therefore, the calculated electrostatic potentials for different surface conditions can be well-aligned in the central bulk region. In Figure 5, we plot the plane-averaged potential for the bare, H−, 50% OH−, and (50% OH + 50% H)-terminated diamond (100) surfaces. All of the potentials agree well inside the bulk and flattened out in the vacuum region, indicating good convergence with respect to the number of diamond layers and the size of the vacuum layers adopted in the calculation. The position of the valence-band maximum EVBM is computed using bulk dia-mond calculations. By adding the experimental band gap $E_g = 5.47$ eV, the position of the conduction-band minimum E_c can be determined. As seen in Figure 5, the clean diamond surface has the largest potential barrier; its vacuum level lies above the conduction band edge E_c, giving an electron affinity of +0.28 eV. The present calculated results for bare and hydrogenated diamond surfaces are consistent with previous work.[37,41,44] Rutter et al. also shows that OH groups on diamond (100) have NEA.[41] With 50% OH + 50% H coverage, the vacuum level is lowered by about 2.86 eV to an electron affinity of −2.59 eV, which is lower than the hydrogenated surface with an electron affinity of −2.32 eV. Some disagreement between the absolute electron affinity values from our DFT calculations and the experimentally measured values is due to parameters like surface coverage. Nevertheless, our DFT calculations have clearly shown that H and OH groups from dissociated water on the diamond surface are responsible for NEA observed in the experiments. Note that our annealed sample after maximum water dosage has the

highest NEA peak in Figure 1b, even though its NEA is still smaller than hydrogenated diamond surface in Table 1. The photoemission intensity is known to be governed by many factors besides NEA, such as band bending and diffusion lengths of electrons and excitons.[45-47] As our sample has an NEA of only about 0.2−0.3 eV higher than hydrogenated diamond and there is still no energy barrier for electron emission, other factors should be dominant in the secondary electron emission intensity.

In conclusion, the NEA condition was produced on diamond when water was adsorbed on bare diamond (100) surface at room temperature, and the observed NEA is comparable to that on hydrogenated diamond. A dipole layer formed by the mixture of OH and CH groups on the diamond surface is responsible for the observed NEA, and this is confirmed by DFT calculations. We have also reported that it is possible to lower the electron affinity by C−H bonds from adsorbed organic molecules attached to the diamond surface;[48] hence, it will be of interest to study organic molecules with O−H groups that could further lower the electron affinity. Such work could pave the way toward surface-functionalized diamond based molecular electronic devices.

References and Notes

(1) Yang, W.; Auciello, O.; Bulter, J. E.; Cai, W.; Carlisle, J. A.; Gerbi, J. E.; Gruden, D. M.; Knickerbocker, T.; Lasseter, T. L. T; Russell, J. N., Jr.; Smith, L. M.; Hamers, R. J. *Nat. Mater.* **2002**, *1*, 253.

(2) Nebel, C. E.; Shin, D.; Takeuchi, D.; Yamamoto, T.; Watanabe, H.; Nakamura, T. *Langmuir* **2006**, *22*, 5645.

(3) Chong, K. F.; Loh, K. P.; Vedula, S. R. K.; Lim, C. T.; Sternschulte, H.; Steinmuller, D.; Sheu, F. s.; Zhong, Y. L. *Langmuir* **2007**, *23*, 5615.

(4) Zhong, Y. L.; Chong, K. F.; May, P. W.; Chen, Z. K.; Loh, K. P. *Langmuir* **2007**, *23*, 5824.

(5) Himpsel, F. J.; Knapp, J. A.; Van Vechten, J. A.; Eastman, D. E. *Phys. Rev. B* **1979**, *20*, 624.

(6) Van der Weide, J.; Zhang, Z.; Baumann, P. K.; Wensell, M. G.; Bernhole, J.; Nemanich, R. J. *Phys. Rev. B* **1994**, *50*, 5803.

(7) Cui, J. B.; Ristein, J.; Ley, L. *Phys. Rev. Lett.* **1998**, *81*, 429.

(8) Maier, F.; Ristein, J.; Ley, L. *Phys. Rev. B* **2001**, *64*, 165411.

(9) Hayashi, K.; Yamanaka, S.; Watanabe, H.; Sekiguchi, T.; Okushi, H.; Kajimura, K. *J. Appl. Phy.* **1997**, *81*, 744.

(10) Looi, H. J.; Jackmann, R. B.; Foord, J. S. *Appl. Phy. Lett.* **1998**, *72*, 353.

(11) Nebel, C. E.; Sauerer, C.; Ertl, F.; Stutzmann, M.; Graeff, C. F. O.; Bergonzo, P.; Williams, O. A.; Jackmann, R. B. *Appl. Phy. Lett.* **2001**, *79*, 4541.

(12) Ristein, J.; Maier, F.; Stammer, M.; Ley, L. *Diamond Relat. Mater.* **2001**, *10*, 416.

(13) Kawarada, H. *Surf. Sci. Rep.* **1996**, *26*, 205.

(14) Kohn, E.; Adamschik, M.; Schmid, P.; Denisenko, A.; Aleksov, A.; Ebert, W. *J. Phy. D: Appl. Phy.* **2001**, *34*, R77.

(15) Kasu, M.; Ueda, K.; Yamauchi, Y.; Makimoto, T. *Appl. Phy. Lett.* **2007**, *90*, 43509.

(16) Garrido, J. A.; Hardl, A.; Kuch, S.; Stutzmann, M.; Williams, O. A.; Jackmann, R. B. *Appl. Phy. Lett.* **2005**, *86*, 073504.

(17) Okano, K.; Koizumi, S.; Ravi, R.; Silva, P.; Amaratunga, G. A. J. *Nature* **1996**, *381*, 140.

(18) Maier, F.; Riedel, M.; Mantel, B.; Ristein, J.; Ley, L. *Phys. Rev. Lett.* **2000**, *85*, 3472.

(19) Foord, J. S.; Lau, C. H.; Hiramatsu, M.; Jackmann, R. B.; Nebel, C. E.; Bergonzo, P. *Diamond Relat. Mater.* **2002**, *11*, 856.

(20) Ley, L.; Ristein, J.; Meier, F.; Riedel, M.; Strobel, P. *Physica B* **2006**, *376*, 262.

(21) Ristein, J. *Science* **2006**, *313*, 1057.

(22) Struck, L. M.; DÉvelyn, M. P. *J. Vac. Sci. Technol. A* **1993**, *11*, 1992.

(23) Reinke, P.; Knop-Gericke, A.; Haävecker, M.; Schedel-Niedrig, Th. *Surf. Sci.* **2000**, *447*, 229.

(24) Laikhtman, A.; Lafosse, A.; Le Coat, Y.; Azria, R.; Hoffman, A. *Surf. Sci.* **2004**, *551*, 99.

(25) Yu, X.-Y.; Wilhelmi, O.; Moser, H. O.; Vidyaraj, S. V.; Gao, X.; Wee, A. T. S.; Nyunt, T.; Qian, H.; Zheng, H. *J. Electron Spectrosc. Relat. Phenom.* **2005**, *114−147*, 1031.

(26) Graupner, R.; Hollering, M.; Ziegler, A.; Ristein, J.; Ley, L.; Stampfl, A. *Phys. Rev. B* **1997**, *55*, 10841.

(27) Diederich, L.; Küttel, O. M.; Ruffieux, P.; Pillo, Th.; Aebi, R.; Schlapbach, L. *Surf. Sci.* **1998**, *417*, 41.

(28) Diederich, L.; Küttel, O. M.; Aebi, P.; Schlapbach, L. *Surf. Sci.* **1998**, *418*, 219.

(29) Thiel, P. A.; Madey, T. E. *Surf. Sci. Rep.* **1987**, *7*, 211.

(30) Henderson, M. A. *Surf. Sci. Rep.* **2002**, *46*, 1.

(31) Makau, N. W.; Derry, T. E. *Surf. Rev. Lett.* **2003**, *10*, 295.

(32) Warren, J. L.; Yarnell, J. L.; Dolling, G. et al. *Phys. Rev.* **1967**, *158*, 805; Alfonso, D. R.; Drabold, D. A.; Ulloa, S. E. *Phys. Rev. B* **1995**, *51*, 1989; Lee, S. T.; Apai, G. *Phys. Rev. B* **1993**, *48*, 2684; Hossain, M. D.; Kubo, T.; Aruga, T. et al. *Jpn. J. Appl. Phys.* **1999**, *38*, 6659.

(33) Parra, R. D.; Zeng, X. C. *J. Chem. Phys.* **1999**, *110*, 6329.

(34) Ando, T.; Inoue, S.; Ishii, M.; Kamo, M.; Sato, Y.; Yamada, O.; Nakano, T. *J. Chem. Soc., Faraday Trans.* **1993**, *89*, 749.

(35) Pehrsson, P. E.; Mercer, T. W. *Surf. Sci. B* **2000**, *460*, 49.

(36) Skokov, S.; Weiner, B.; Frenklach, M. *Phys. Rev. B* **1997**, *55*, 1895.

(37) Sque, S. J.; Jones, R.; Briddon, P. R. *Phys. Rev. B* **2006**, *73*, 85313.

(38) Stöhr, J. *NEXAFS Spectroscopy*; Springer: Berlin, 1992.

(39) Nagasaka, M.; Nakai, I.; Kondoh, H.; Ohta, T.; Carravetta, V. *Chem. Phys. Lett.* **2003**, *375*, 419.

(40) Amemiya, K.; Kitajima, Y.; Yonamoto, Y.; Terada, S.; Tsukaba-yashi, H.; Yokoyama, T.; Ohta, T. *Phys. Rev. B* **1999**, *59*, 2307.

(41) Rutter, M. J.; Robertson, J. *Phys. Rev. B* **1998**, *57*, 9241.

(42) Kresse, G.; Furthmüller, J. *Phys. Rev. B* **1996**, *54*, 11169; Kresse, G.; Furthmüller, J. *Comput. Mater. Sci.* **1996**, *6*, 15.

(43) Vanderbilt, D. *Phys. Rev. B* **1990**, *41*, R7892.

(44) Zhang, Z.; Wensell, M.; Bernholc, J. *Phys. Rev. B* **1995**, *51*, 5291.

(45) Bandis, C.; Pate, B. B. *Phys. Rev. Lett.* **1995**, *74*, 777.

(46) Bandis, C.; Pate, B. B. *Phys. Rev. B* **1995**, *52*, 12056.

(47) Ristein, J.; Stein, W.; Ley, L. *Phys. Rev. Lett.* **1997**, *78*, 1803.

(48) Ouyang, T.; Gao, X.; Qi, D.; Wee, A. T. S.; Loh, K. P. *J. Phys. Chem. B* **2006**, *110*, 5611.